The 2015 World Congress on
Advances in Structural Engineering and Mechanics (ASEM15)
Incheon, Korea, August 25-29, 2015

A Study on Structural Performance of Composite Column using the L-shaped molded steel and Template to Lattice Composite Beam for Slim Floor Connection

*Kyong-Soo Yom[1)], Duck-Ki Pyo[2)] and *Sung-Mo Choi[1)]

[1)] Harmony Structural Engineering, Seoul, Korea
[2),3)] Department of Architectural Engineering, University of Seoul, Korea
[3)] smc@uos.ac.kr

ABSTRACT

This study suggests new types of column-to-beam connections each of which consists of a new-shaped composite column and a beam. The structural performance of the new column-to-beam connections is evaluated by loading tests. The column used in the suggested column-to-beam connections is the RC column whose corners are reinforced with L-shaped steel members. The RC beam used in the connections is composed of L-shaped steel members, truss webs and a bottom plate. Four column-to-beam connection specimens were fabricated for loading tests to observe structural performance. Three of them were tested under cyclic load and one was tested under monotonic load. Among the specimens, the one which was fabricated in accordance with the KBC 2009 seismic design details satisfied the seismic requirements for special moment frames prescribed in the KBC 2009.

Keyword: New shape, Composite column, Composite beam, Structural performance, Column to beam connection, Seismic connection

1. Introduction

High-rise and large-scale buildings have required and boosted the development of new structural members. The steel tube of a concrete filled steel tube (CFT) column deals with tensile force and the concrete inside the tube deals with compressive force. Since the steel tube confines the concrete and the concrete restrains the local buckling of the tube, CFT columns have high strength and energy absorption. But, CFT columns also have disadvantages. When the cross-section of the column is large, large width-thickness ratio causes a complication to fabrication and construction process. The closed cross-section of the column provides a narrow choice of column-

---

[1)] Head of Office(Presenter)
[2)] Master Course
[3)] Professor

to-beam connections. This study suggests new-shaped composite column to new-shaped composite beam connections and provides equations. The details of the connections were developed to deal with both vertical load and seismic load. The suggested equations were verified through the evaluation of behavioral characteristics, structural performance and seismic performance of the connections.

2. Development of connection details

2.1 Composite beam

The new-shaped composite beam is a reinforced concrete-filled beam which has advantages such as reduced steel amount and reduced floor height. In addition, it does not require supporting posts for concrete casting. The truss webs and the bottom plate of the beam shown in figure 1 make various PC floor plates such as HCS and deep deck available. After the steel frame of the beam is fabricated, it is moved to the field, where concrete is cast.

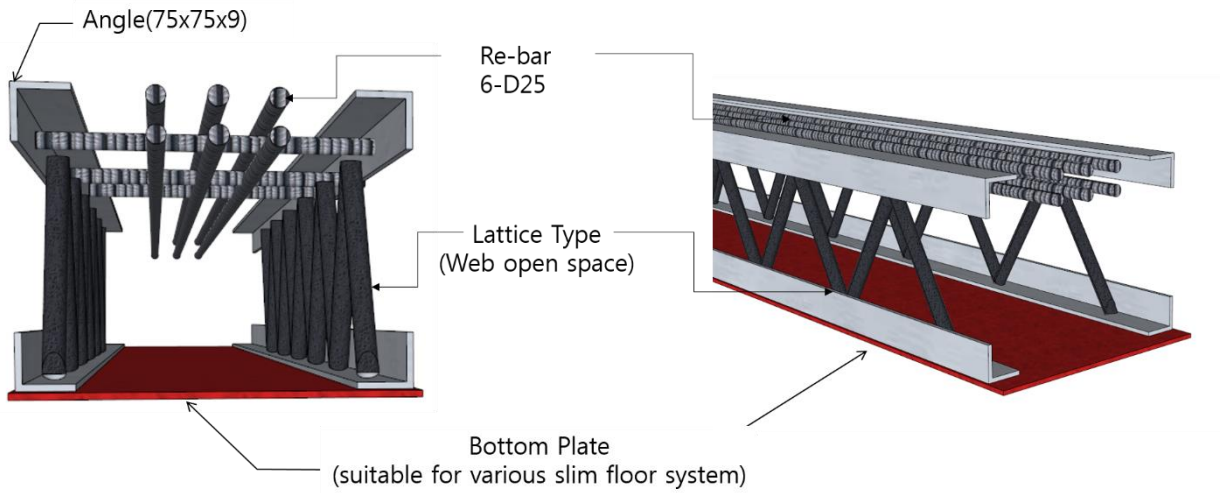

(a) ANI Girder diagram

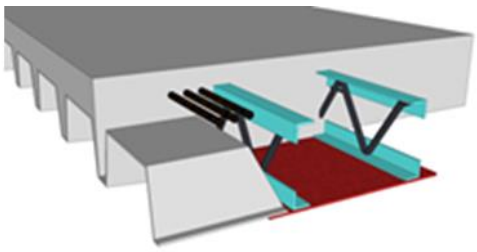

(b) Deep Deck

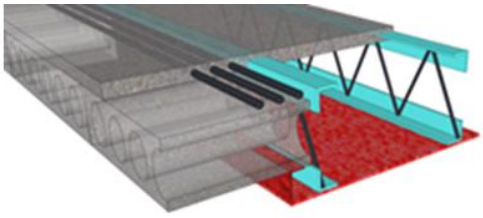

(c) Hollow Core Slab

Fig. 1 Proposed New type Composite Beam

2.2 Composite column

The fabrication of the new-shaped composite column suggested in this study does not require molds. In addition, structurally excellent large-section columns can be realized

and vertical re-bars are placed at the factory. Since the column has closed cross-sections, the number of molds is reduced. A bracket is welded to the column so that a precast type composite beam is easily placed. The column has an open space for casting concrete and installing re-bars. Figure 2 shows the details of the column.

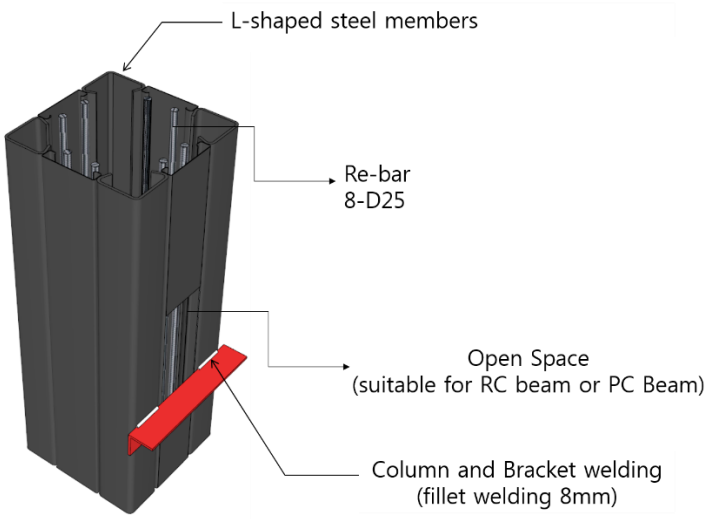

Fig. 2 Proposed New type Composite Beam

2.3 Connection details

The new composite beam is placed at the column bracket and the bottom plate of the beam is welded to the column bracket. As shown in figure 3, the process requires minimum welding. Rebars (6-D25) are placed at the upper part of the beam. The upper L-shaped steel members of the beam are 120mm apart from the column in order for the rebars to deal with stress when vertical load is applied as well as for convenience's sake. The equations for the connection were suggested for the verification of structural performance. It was also judged whether the throat depth of lower part welding and the details of the upper part were feasible for field application.

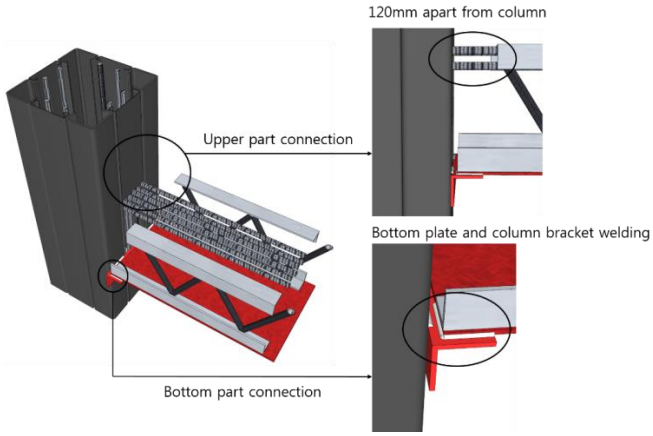

Fig. 3 Proposed Connection Detail

3. Equations of the connection

The whole cross-sections of a complete composite beam exhibit bending performance when the horizontal shear strength of shear connectors is greater than the strength of the concrete or steel, whichever is smaller. The ultimate strength of a complete composite beam under positive moment and negative moment can be estimated based on the plastic analysis using the equivalent stress block of concrete prescribed in the KBC 2009. The moment equations for the specimens were suggested and verified by tests.

Table. 1 Negative, Positive stress distribution of Proposed connection(CNN)

Negative	Positive
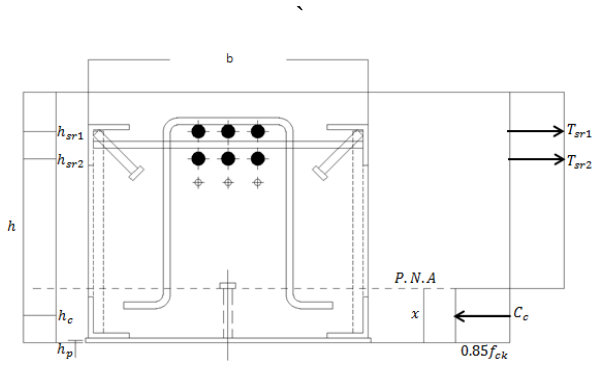	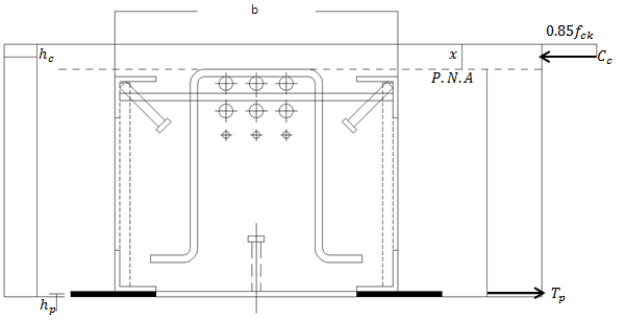
Negative moment	$\mathrm{C} = C_c$ $\mathrm{T} = T_{sr1} + T_{sr2}$
Positive moment	$\mathrm{C} = C_c$ $\mathrm{T} = T_p$

Table 1 shows stress distribution in specimen CNN. The value of x, the distance between compressive axis and neutral axis, was estimated under equilibrium condition of C=T. For the specimen, the negative stress is given by the following equation (1).

$$\mathrm{M} = \mathrm{T_{sr1}} \times (\mathrm{h} - \mathrm{x} - \mathrm{h_{sr1}}) + \mathrm{T_{sr2}} \times (\mathrm{h} - \mathrm{x} - \mathrm{h_{sr2}}) + \mathrm{C_c} + \mathrm{h_c} \quad (1)$$

The positive moment for the specimen is given by equation (2).

$$\mathrm{M} = \mathrm{T_p} \times (\mathrm{h} - \mathrm{x} - \mathrm{h_p}) + \mathrm{C_c} + \mathrm{h_c} \quad (2)$$

The strength of the specimens was estimated using the plastic stress distribution of steel and concrete prescribed in the KBC 2009 0709. Table 2 shows the positive moment ($\mathrm{M_n}$) and negative moment ($\mathrm{P_n}$) of the specimens.

Table. 2 Design strength

		M_n(kN·m)	P_n(kN)
CNN	Positive	352.99	100.85
	Negative	492.35	140.67
CWN	Positive	352.99	100.85
	Negative	607.58	173.59
UNN	Negative	492.35	140.67
CNR	Positive	343.45	98.12
	Negative	492.35	140.67

4. Structural performance evaluation

4.1 Test plan

Four specimens were fabricated for structural performance tests as shown in table 3. Variables were the cross-sectional shape of the composite beam, throat depth and loading type. In basic specimen CNN, 6 rebars (D25) were placed in 2 rows at the upper part of the beam and the column bracket and the beam bottom plate were joined by 5mm fillet welding. In specimen CWN, 6 rebars (D25) were placed in 2 rows at the upper part of the beam and the column and the upper L-shaped steel members of the beam were 10mm groove-welded. While specimen UNN and specimen CNN had the same details, the former was tested under monotonic load. In specimen CNR, 3 rebars (D25) were placed at the lower part of the beam as prescribed in the KBC 2009 seismic details. Table 3 shows the details of the specimens.

Table. 3 Specimen List

NO.	Specimen	Upper part of beam reinforced	Lower part of the beam reinforced	Upper part welded (column-beam)	Bottom part welded (column bracket-beam bottom plate)	Loading patten
1	CNN	6-D25	-	-	Fillet welded(5mm)	cyclic
2	CWN	6-D25	-	**Groove welded (10mm)**	**Groove welded (10mm)**	cyclic
3	UNN	6-D25	-	-	Fillet welded (5mm)	**under**
4	CNR	6-D25	**3-D25**	-	Fillet welded (3mm)	cyclic

C(U)-W(N)-R(N)

Lower part of the beam, R ; Reinforcement
N ; No Reinforcement

Groove welded of beam upper part, W ; Welded
N ; No Welded

Loading patten, C ; Cyclic Loading
U ; Under Loading

a. CNN-bottom welded
(fillet welded 5mm)

b. CWN-upper groove welded(10mm)

c. CNR- bottom welded
(fillet welded 3mm)

d. CNR-lower part of the beam
reinforcement(3-D25)

Fig. 4 Specimen Detail

4.2 Test setup

Figure 5 shows the setup for the tests. A 2,000kN actuator was used for cyclic loading and the distance between the loading point and column's center was 3,500mm. In order to prevent the out-of-plane deformation of the beam, lateral buckling prevention posts were placed at the two sides of the beam near loading point. The KBC 2009 cyclic loading program for seismic performance evaluation shown in figure 5 was used.

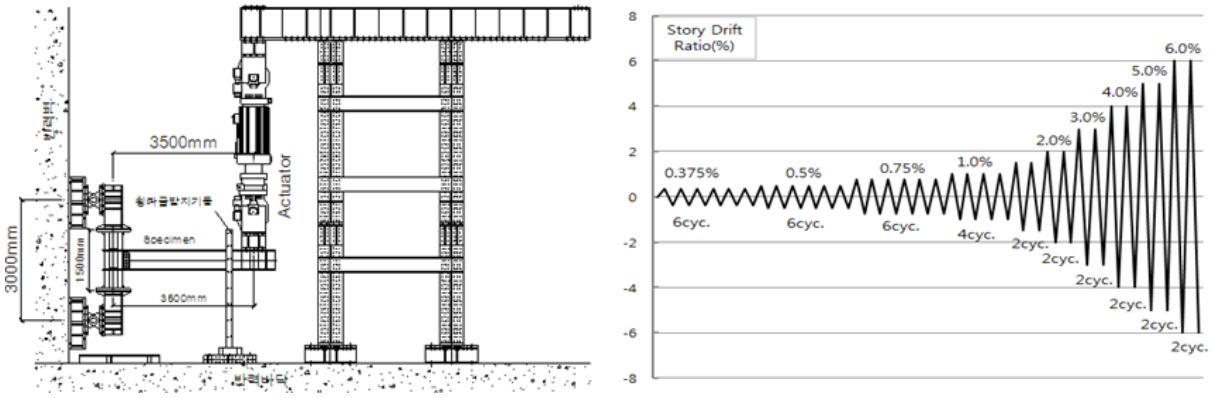

a. Boundary condition b. KBC 2009 Cyclic Loading Program

Fig. 5 Boundary condition and Loading program

4.3 Test result and analysis

4.3.1 Load-displacement relation

Figure 6 shows the load-displacement relation of the specimens under cyclic load and monotonic load. X axis and Y axis mean beam displacement and load, respectively. When downward load was applied, the maximum load of specimen CNN was smaller than the estimation (P_n), while the maximum load of specimens CWN, UNN and CNR was greater than the estimation (P_n). When upward load was applied, the maximum load of specimens CNN, CWN and CNR was greater than the estimation (P_n). Specimen UNN maintained ductility after yield. Specimen CNR which was fabricated in accordance with the KBC 2009 seismic details exhibited ductile behavior after yield under both upward load and downward load. Specimen CWN maintained high load capacity under downward load, while weld failure was observed and load capacity deteriorated significantly under upward load.

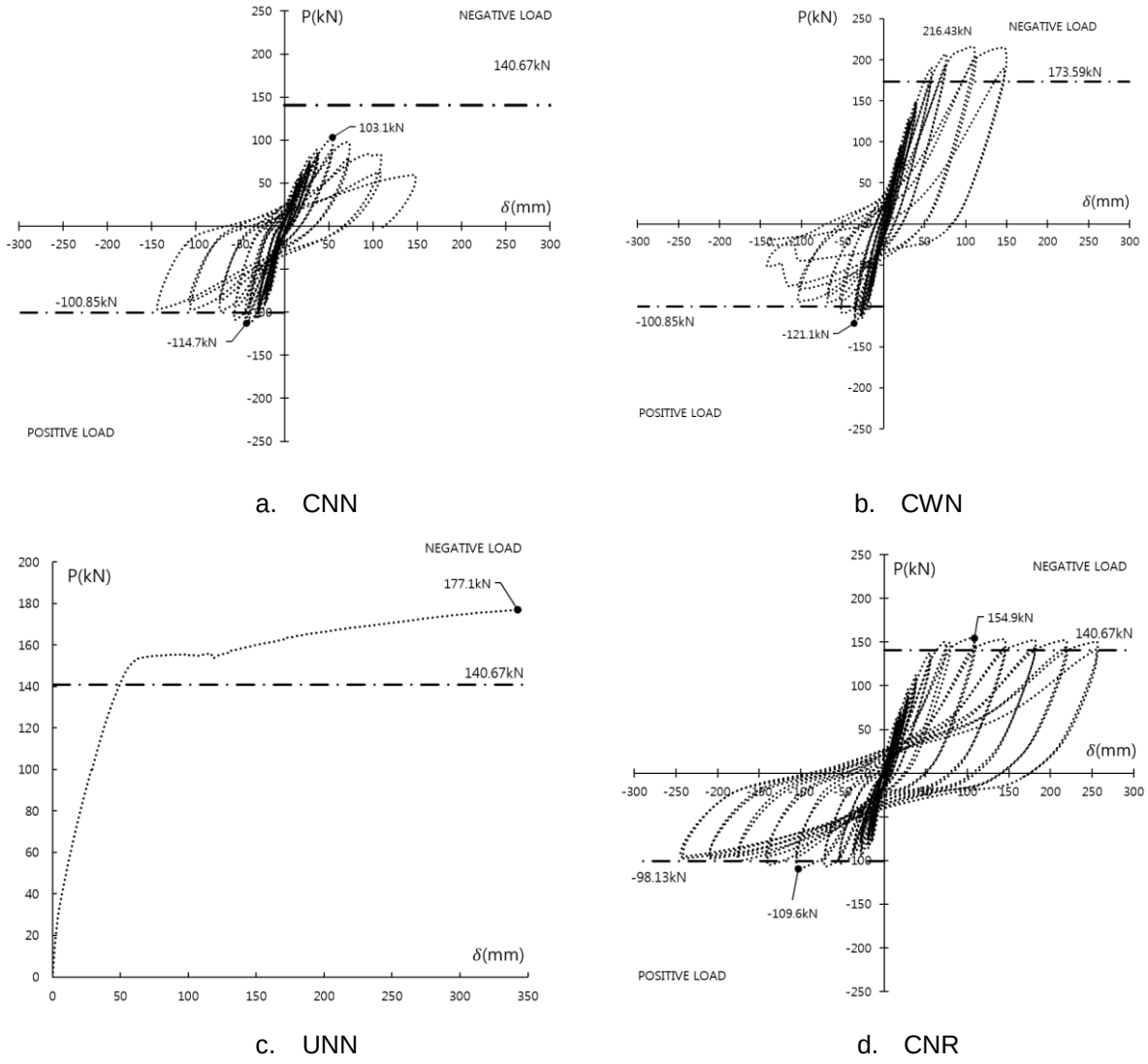

Fig. 6 Load-displacement curve relationship

4.3.2 Failure mode

Figure 7 shows the failure modes of the specimens. In specimens CNN and CWN whose lower parts were not reinforced with rebars, column-bracket weld started to fail from step 5 as shown in figure 6(a) under upward load. In specimen UNN, the central part the concrete where the rebars were placed ruptured as shown in figure 6 (b), implying stress concentration in the center of the beam. Figure 7 (c) shows weld failure at the joint of column bracket and beam bottom plate in specimen CWN. It displayed ductile behavior until weld failure, after which load capacity deteriorated rapidly. Figure 6 (d) shows weld failure at the joint of column bracket and beam bottom plate in specimen CNR which was fabricated in accordance with the KBC 2009 seismic design details. While the specimen experienced the slight deterioration of load capacity after weld failure, the lower rebars dealt with the load to exhibit ductile

behavior.

a. CNN, CWN column bracket : Weld failure

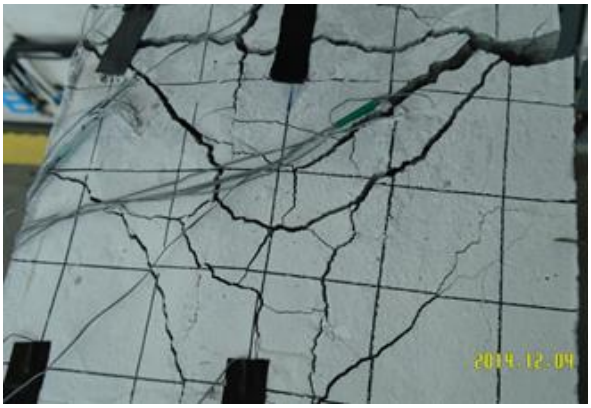

b. UNN upper part concrete : Concrete failure

c. CWN bottom plate : Weld failure

d. CNR bottom : Weld failure

Fig. 7 Specimen main failure mode

4.3.3 Initial stiffness

Figure 9 shows the positive and negative initial stiffness of the specimens. The initial stiffness of specimen CWN where the column and the upper L-shaped steel members of the beam were butt-welded was 1.4~1.7 times higher than that of other specimens because not only the upper rebars but also the upper L-shaped steel members dealt with stress. The line graphs in figure 8 show the slopes of initial stiffness. Figure 9 show the numerical comparison of initial stiffness. Positive initial stiffness was 1.5 times higher than negative initial stiffness, which implied that greater tensile force was applied to steel members at the initial stage of loading. The deterioration of load capacity after weld failure implies that rebars exert great influence on ductility.

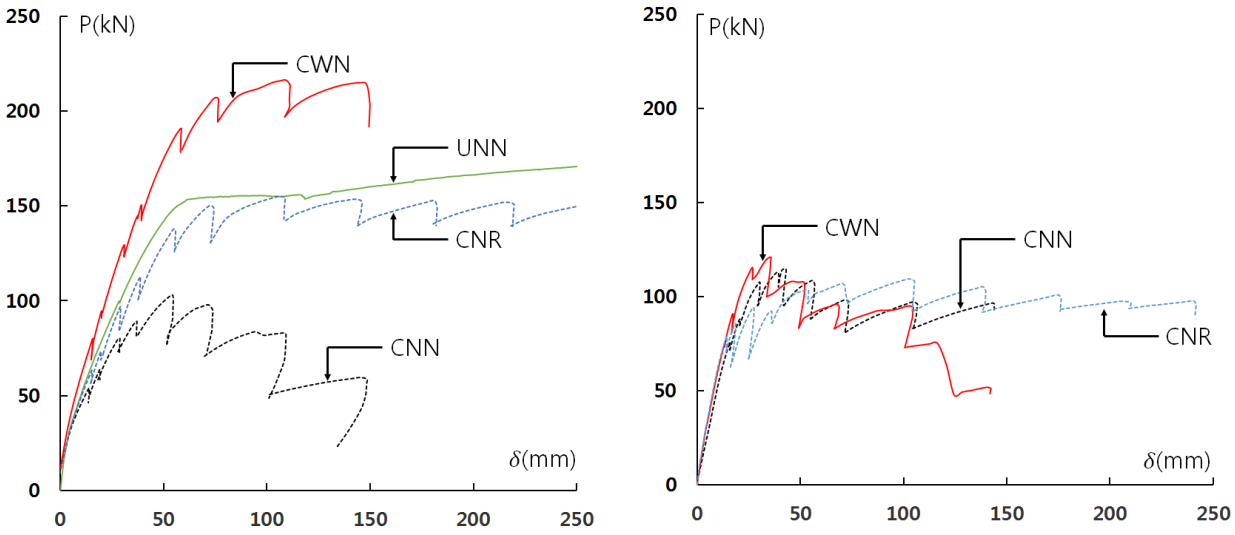

Fig. 8 Skeleton P- δ Curve of Each Specimen

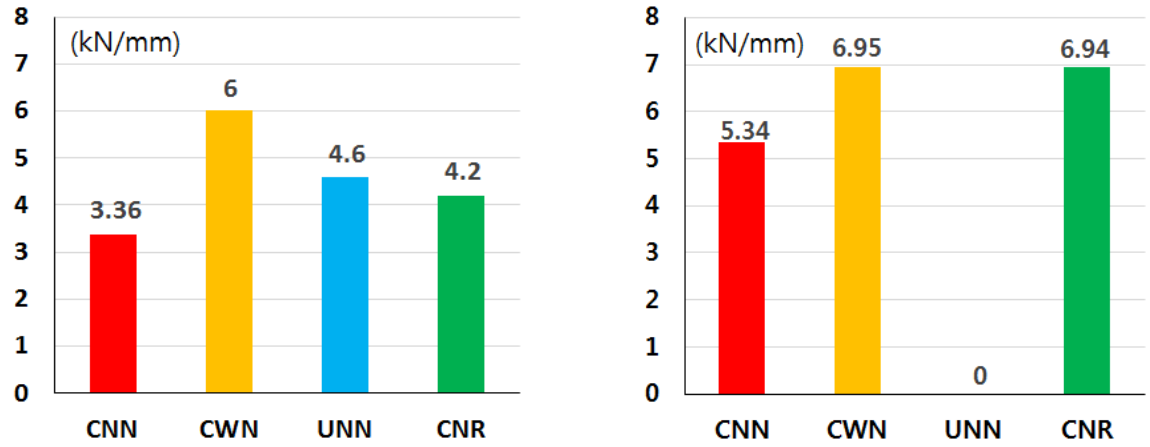

Fig. 9 Comparison of initial stiffness each specimens

4.3.4 Ultimate strength

Table 2-11 and figure 2-29 show estimated strength (P_{ut}) obtained by the equation mentioned above and ultimate strength (P_{ue}) obtained by the tests. In all of the specimens, ultimate strength was close to the estimation. The ultimate strength of specimen CNN was 36% lower than the estimation because the upper rebars did not yield. In specimen CWN where the column and the upper L-shaped steel members of the beam were butt-welded, not only the rebars but also the upper steel members dealt with stress when downward load was applied. The ultimate strength of the specimen was 216.4kN, which was 24% higher than the estimation. It was 22~53% higher than 114.7kN of CNN, 177.1kN of UNN and 154.9kN of CNR. In CNR specimen reinforced

with both upper and lower rebars as advised by the KBC 2009 seismic design details, the lower rebars dealt with most of upward load after weld failure.

Table. 4 Compariosn of Design strength and Ultimate strength

		P_{ut}(kN)	P_{ue}(kN)	P_{ue}/P_{ut}
CNN	Positive	100.85	114.7	1.14
	Negative	140.67	103.1	0.73
CWN	Positive	100.85	121.1	1.20
	Negative	173.59	216.4	1.24
UNN	Negative	140.67	177.1	1.26
CNR	Positive	98.12	109.6	1.12
	Negative	140.67	154.9	1.10

4.3.5 Deformation capacity

Yield load is defines as the intersection of line A which is tangential to load-displacement curve and line B which has 1/3 slope of line A and is tangential to the curve. The deflection at the point is defined as yield displacement (δ_y). Table 5 shows the yield load, yield displacement, ultimate strength and ultimate displacement of the specimens.

Table. 5 Yeild strength, Yeild displacement, Ultimate strength, Ultimate displacement of each specimen

		P_y(kN)	δ_y(mm)	P_u(kN)	δ_u(mm)
CNN	Positive	76.57	25.9	114.7	42
	Negative	85.71	19.25	103.1	39.03
CWN	Positive	82.85	15.4	121.1	35
	Negative	118	26.95	216.4	108.5
UNN	Negative	450	56.54	177.1	345
CNR	Positive	77.14	12.25	109.6	101.5
	Negative	104.28	35	154.9	108.5

Deformation capacity is defined as the ratio of maximum displacement to yield displacement (δ_u/δ_y). The deformation capacity of the basic specimen tested under monotonic load was greater than that of the specimens under cyclic load. The deformation capacity of the specimen where the column and the upper L-shaped steel members of the beam were butt-welded was greater than that of the specimen whose upper parts were not welded. When upward load was applied, specimen CNR where rebars were placed at the lower part of the beam exhibited greater deformation capacity than that without lower reinforcement. Figure 10 shows the deformation capacity of the specimens.

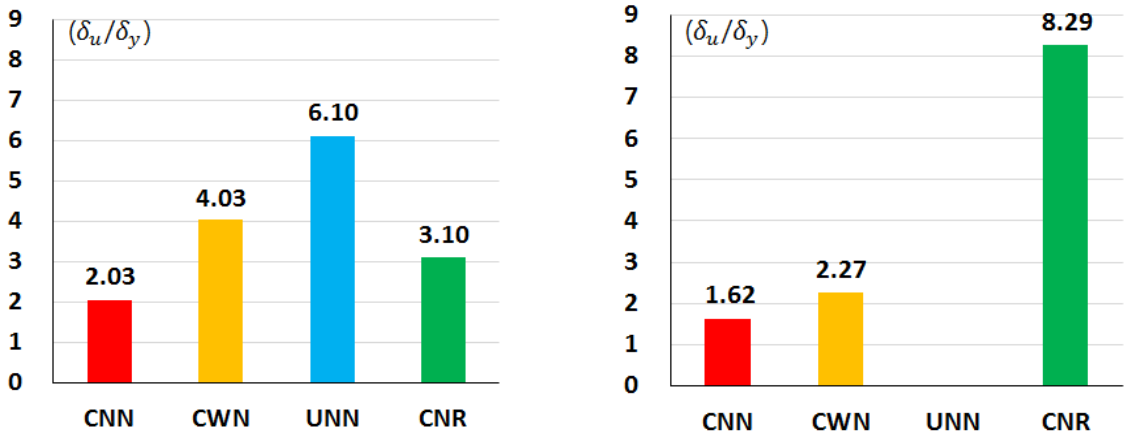

(a) Negative (b) Positive

Fig. 10 Deformation Capacity : δ_u/δ_y ratio

5. Conclusions

In this study, new types of composite column-to-beam connections and the equations for the connections were suggested. One of the column-to-beam connection specimens was fabricated in accordance with the KBC 2009 seismic design details. The evaluation of the structural performance of the new column-to-beam connections provided the following conclusions.

(1) The maximum strength of the specimens was 10~24% greater than the estimation obtained by the equation, which implies that the new types of composite column-to-beam connections are reliable and can be applied to structural designs.

(2) The specimen where the lower part of the beam was reinforced with rebars as prescribed in the KBC 2009 seismic design details displayed ductile and stable behavior without brittle fracture. The bending strength of the specimen was 80% of nominal plastic bending strength (M_n) or above and story deformation angle was 0.04rad.

(3) Specimen UNN tested under monotonic load displayed excellent deformation capacity when vertical load was applied. The deformation capacity of specimen CWN where both upper and lower joints were butt-welded was 1.3 times greater than that of basic specimen CNN. The deformation capacity of specimen CNR where the lower part of the beam was bar-reinforced was 3.6~5.1 times greater than that of the specimens without lower reinforcement.

(4) The strength of specimen CWN where both upper and lower joints were butt-welded was greater than that of basic specimen CNN because the upper L-shape steel members also dealt with stress. The welded joint of the column bracket and beam bottom plate in specimen CWN ruptured when upward load was applied.

The new types of composite column-to-beam connections turned out to be feasible.

The specimen where the lower part of the beam was rebar-reinforced in accordance with the KBC 2009 seismic design details satisfied the seismic requirements for special moment frames. The composite column-to-beam connections suggested in this study can be a yardstick by which the throat depth and details of column-to-beam connections in different settings are decided.

ACKNOWLEDGEMENTS

This research (Grants No. 201406172002) was supported by Business for Cooperative R&D between Industry, Academy, and Research Institute funded Korea Small and Medium Business Administration in 2014.

REFERENCES

Marcela N. Kataoka, Ana Lucia H.C. El Debs (2014), "Parametric study of composite beam-column connections using 3D finite element modelling", *J. Mat. Civil Eng., JCSR,* Vol.102, 136-149.

Kim, S.B., Kim, S.S. and Ryu, D.S. (2013), "Study on the Cyclic Seismic Testing of U-shape Hybrid Composite Beam-to-Composite Column Connections", *J. Mat. Civil Eng., KCI,* Vol.25 No.1, 47-59.

Lee, S.H. (2008), "Behavior of Welded Built-up Square CFT Columns and Connections", *Paper of Doctor's degree*

Park, S.H. (2004), "A Study on the structural capacities for CFT square column-to-beam partially restrained composite connections", *Paper of Master's degree*